SCIENTIFIC REPORTS

OPEN

SUBJECT AREAS:
HETEROGENEOUS CATALYSIS
CATALYTIC MECHANISMS
MASS SPECTROMETRY
SURFACE SPECTROSCOPY

Received
14 February 2013

Accepted
26 March 2013

Published
9 April 2013

Correspondence and requests for materials should be addressed to W.X.H. (huangwx@ustc.edu.cn) or F.Q. (fqi@ustc.edu.cn)

Methyl Radicals in Oxidative Coupling of Methane Directly Confirmed by Synchrotron VUV Photoionization Mass Spectroscopy

Liangfeng Luo[1,2,3], Xiaofeng Tang[4], Wendong Wang[2,3], Yu Wang[4], Shaobo Sun[4], Fei Qi[4] & Weixin Huang[1,2,3]

[1]Hefei National Laboratory for Physical Sciences at the Microscale, University of Science and Technology of China, Hefei 230026, China, [2]CAS Key Laboratory of Materials for Energy Conversion, University of Science and Technology of China, Hefei 230026, China, [3]Department of Chemical Physics, University of Science and Technology of China, Hefei 230026, China, [4]National Synchrotron Radiation Laboratory, University of Science and Technology of China, Hefei 230029, China.

Gas-phase methyl radicals have been long proposed as the key intermediate in catalytic oxidative coupling of methane, but the direct experimental evidence still lacks. Here, employing synchrotron VUV photoionization mass spectroscopy, we have directly observed the formation of gas-phase methyl radicals during oxidative coupling of methane catalyzed by Li/MgO catalysts. The concentration of gas-phase methyl radicals correlates well with the yield of ethylene and ethane products. These results lead to an enhanced fundamental understanding of oxidative coupling of methane that will facilitate the exploration of new catalysts with improved performance.

Oxidative coupling of methane (OCM) has remained as one of the great but rewarding challenges within heterogeneous catalysis research since the pioneering work of Keller and Bhasin[1]. A large economical interest in the OCM reaction, as well as the associated supremely challenging scientific aspects, has ensured this topic's high popularity over the preceding decades[2–6]. The goal of OCM catalysts is to achieve a high selectivity to ethane and ethylene (C_2 products) at a high methane conversion, with an overall C_2 yield of 30%[7]. Meanwhile, OCM reactions generally take place at 650–800°C to activate the strong C–H bond in methane, the stability of OCM catalysts is also a great challenge. Although a large number of compounds have been tried, OCM catalysts are still quite far away from the economical target. Therefore, the exploration of new catalytic materials must be based on the fundamental question of which properties a well-performing OCM catalyst should possess. It is thus of high importance and significant scientific interest to elucidate the reaction mechanism and structure-activity relationship at the molecular level.

The OCM reaction is proposed to be initiated via the activation of methane on the catalyst surface to generate methyl radicals, and the secondary reactions of methyl radicals either on the catalyst surface or in the gas phase lead to the C_2 products[5,7], however, due to the lack of routine techniques for the detection of methyl radicals, solid experimental evidence for such a OCM reaction mechanism is very rare[8–18]. Using a matrix isolation electron spin resonance (MIESR) system, Lunsford et al. have detected surface-generated, gas-phase methyl radicals in the OCM reaction catalyzed by various catalysts[8–17], but MIESR is not a technique capable of directly detecting gas-phase radicals. Schlögl's group developed molecular-beam mass spectroscopy with threshold ionization using the electron impact ionization technique for the in-situ investigation of gas-phase transient intermediates in heterogeneous catalytic reactions[19,20]. Recently synchrotron VUV photoionization combined with molecular-beam mass spectroscopy, also referred as synchrotron VUV photoionization mass spectroscopy (SVUV-PIMS), was developed to study low-pressure premixed laminar flames[21]. Comparing with electron impact ionization, synchrotron VUV photoionization possesses the advantages of wide tunability and high energy resolution and thus can minimize fragmentation interference, distinguish isomers, and detect radicals. The application of SVUV-PIMS has achieved great success in detecting combustion intermediates and comprehensive measurement of flame structure for combustion studies[22–24]. Several reports also extended the application of SVUV-PIMS to heterogeneous catalytic reaction systems and chemical vapor deposition systems[25–27]. In this paper, we report

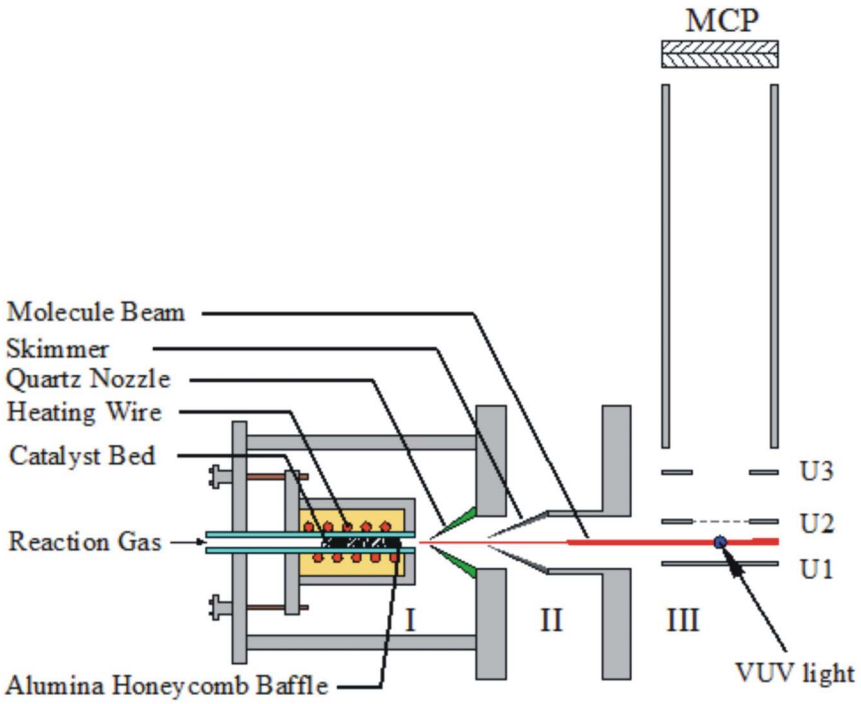

Figure 1 | **Scheme of the SVUV-PIMS system online coupled to a catalytic reactor.**

our successful approach to use SVUV-PIMS for the in-situ detection of gas-phase methyl radicals in the OCM reaction. Our results for the first time provide direct experimental evidence for the OCM reaction mechanism. Specially we show, that the reaction is initiated via activation of methane on the catalyst surface to generate methyl radicals.

Results

We designed an online catalytic reactor connected to the SVUV-PIMS system housed in National Synchrotron Radiation Laboratory (Hefei, China)[24]. The experimental set-up is schematically illustrated in Figure 1 and consists of three parts: (I) a catalytic reactor that can be heated up to ~900°C; (II) a differentially pumped chamber; (III) the SVUV-PIMS system with a homemade time-of-flight mass spectrometer[28,29]. The SVUV-PIMS system covers the photon energies from 7.8 to 24.0 eV and is capable of online detecting the gas-phase components of catalytic reactions operated at a total pressure up to 5~6 Torr.

The OCM catalyst used in our study is Li-doped MgO catalyst, one of the most intensively studied OCM catalysts[3,5]. Two types of Li-doped MgO catalysts with calculated Li amount of 1.3% and 5.6% (denoted as 1.3%-Li/MgO and 5.6%-Li/MgO) were prepared by adequately mixing of MgO and Li_2CO_3 finally subjected to calcination in a Muffle furnace at 800°C for 4 hours. Only diffraction patterns arising from MgO were observed in the XRD spectra of as prepared Li/MgO catalysts (Figure S1). Table 1 summarizes specific surface areas and elemental compositions of Li/MgO catalysts. The specific surface area of 1.3%-Li/MgO and 5.6%-Li/MgO catalysts is 15.3 and 2.2 m^2/g, respectively. The Li amount in 1.3%-Li/MgO and 5.6%-Li/MgO catalysts is only 0.21% and 1.16%, respectively. This indicates that Li/MgO catalysts suffer heavy losses of Li during the calcination process, agreeing with previous observations[30,31]. The catalytic performance of Li/MgO catalysts in the OCM reaction was firstly evaluated in an ambient-pressure fixed-bed flow reactor. The catalysts were activated in pure O_2 at 450°C for 2 hours prior to the catalytic performance evaluation. As shown in Figure 2A, both Li/MgO catalysts are active in catalyzing the OCM reaction. 5.6%-Li/MgO catalyst is much more active than 1.3%-Li/MgO catalyst. At 750°C, the CH_4 conversion rate is 10.7 and 84.4 $\mu mol \cdot min^{-1} \cdot m^{-2}$ for 1.3%-Li/MgO and 5.6%-Li/MgO, respectively; and the C_2 selectivity is 33.2% and 44.4% for 1.3%-Li/MgO and 5.6%-Li/MgO, respectively. Both catalysts are stable in catalyzing the OCM reaction under the investigated conditions (Figure 2B).

The OCM reaction catalyzed by both catalysts was then operated in the online catalytic reactor connected to the SVUV-PIMS system at a total reactant pressure of 4 Torr. Figure 3A shows SVUV-PIMS spectra of the gas-phase components of OCM reaction catalyzed by 5.6%-Li/MgO catalyst at 750°C ionized with photons at different energies. Ionized with photons at 10.0 eV, only a single peak with m/z = 15 appears in the SVUV-PIMS spectrum. With the increase of photon energy to 11.6 eV, in addition to the peak at m/z = 15, strong peaks appear at m/z = 28, 30 and 32 in the SVUV-PIMS spectrum. With the further increase of photon energy to 14.0 eV, main peaks appear at m/z = 16, 18, 28 and 32 in the SVUV-PIMS spectrum, but peaks at m/z = 29, 30 and 44 are also visible. No signal was detected by SVUV-PIMS ionized with photons at 9.5 eV (Figure S2), demonstrating that no gas-phase product was formed with its ionization threshold below 9.5 eV. The most important feature of SVUV-PIMS is the measurement of the photoionization efficiency (PIE) spectrum for the targeted m/z signal detected in the SVUV-PIMS spectrum[24]. The PIE spectrum is able to give the ionization threshold of the targeted m/z signal that can unambiguously identify the corresponding gas-phase compound by comparing with standard database such

Table 1 | Compositions and specific surface areas of various Li/MgO catalysts

Catalyst	C_{Li}[a] (wt%)	C_{Li}[b] (wt%)	C_{Li}[c] (wt%)	S_{BET} (m^2/g)
1.3%-Li/MgO	0.21	0.17	0.18	15.3
5.6%-Li/MgO	1.16	0.17	0.15	2.2

[a]: as-prepared Li/MgO catalysts.
[b]: as-prepared Li/MgO catalysts treated in pure O_2 at 450°C for 2 hours.
[c]: as-prepared Li/MgO catalysts after the catalytic performance evaluation in the OCM reaction up to 750°C.

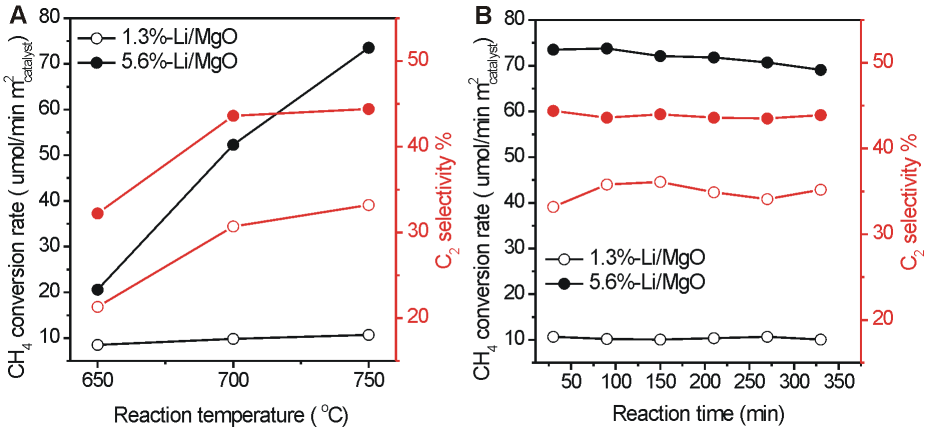

Figure 2 | (A) Catalytic performance of 1.3%-Li/MgO and 5.6%-Li/MgO catalysts in OCM reaction at ambient pressure. (B) Catalytic Stability of 1.3%-Li/MgO and 5.6%-Li/MgO catalysts in OCM reaction at 750°C and ambient pressure.

as NIST online database[32]. Figure 4 shows the PIE spectra of m/z = 15, 16, 18, 28, 30 and 44 detected in the SVUV-PIMS spectra of the gas-phase components of OCM reaction catalyzed by 5.6%-Li/MgO at 750°C. The m/z = 15 signal gives an ionization threshold of 9.80 eV (Figure 4A) that agrees well with the ionization threshold of methyl radicals[32]. Thus this species can be unambiguously identified to be methyl radical (CH_3•). No methyl radical was detected by SVUV-PIMS for the catalytic reaction at 750°C without Li/MgO catalysts (Figure 5A). Meanwhile, no signal except m/z = 40 (Ar) was observed when 5.6%-Li/MgO catalyst was tested at 750°C under the Ar flow (Figure S3). These observations provide direct and solid experimental evidence for the formation of gas-phase methyl radicals during the catalytic OCM reaction and clearly prove that the detected gas-phase methyl radicals are generated by the activation of methane on the Li/MgO catalyst surface. The m/z = 16 signal gives an ionization threshold of 12.60 eV (Figure 4B) and thus can be unambiguously identified to methane (CH_4). The m/z = 28 signal gives two ionization thresholds of 10.47 and 14.10 eV (Figure 4C) respectively corresponding to ethylene (C_2H_4) and carbon monoxide (CO). The observed inflection at ~12.2 eV in Figure 4C corresponds to the $^2B_{3g}$ electronic state of $C_2H_4^+$ ion[33]. The m/z = 30 signal gives two ionization thresholds of 10.86 and 11.53 eV (Figure 4D) respectively corresponding to formaldehyde (HCHO) and ethane (C_2H_6). The observed inflection at ~12.5 eV in Figure 4d corresponds to the ^2E_g electronic state of $C_2H_6^+$ ion[34]. The m/z = 32 signal gives two ionization thresholds of 10.82 and 12.05 eV (Figure 4E) respectively corresponding to methanol (CH_3OH) and oxygen (O_2). The m/z = 44 signal gives an ionization threshold of 13.84 eV (Figure 4F) corresponding to carbon dioxide (CO_2). The m/z = 29 signal in the SVUV-PIMS spectrum acquired with photon energy of 14.0 eV results from the fragmentation of C_2H_6 due to the photodissociation of one C-H bond that requires a photon energy of 12.40 eV[35]. Thus identified by SVUV-PIMS, the gas-phase components of the OCM reaction catalyzed by Li-MgO catalysts include not only methane, oxygen, methyl radical, ethylene, ethane, carbon monoxide, carbon dioxide, but also formaldehyde and methanol. Formaldehyde and methanol were previously reported as trace products of OCM reaction catalyzed by Li/MgO catalysts[36].

Besides gas-phase methyl radical, other likely species with m/z of 15 included gas-phase Li_2H with the ionization threshold is 4.5 eV[29], but its formation can be excluded by the experimental observation that no signal was detected by SVUV-PIMS ionized with photons at 9.5 eV (Figure S2). Thus the m/z = 15 peak in the SVUV-PIMS spectra ionized with photons at 10.0 eV is exclusively contributed by gas-phase methyl radical and its peak intensity represents the gas-phase concentration of methyl radical. The gas-phase concentration of ethylene can be represented by the integrated intensity of the m/z = 28 peak in the SVUV-PIMS spectra ionized with photons at 11.6 eV. The m/z = 30 peak in the SVUV-PIMS spectra ionized with photons at 11.6 eV is contributed by ethane and formaldehyde, and the ethane/formaldehyde ratio can be calculated from the corresponding PIE spectrum[37]. Figure S4 shows SVUV-PIMS spectra of

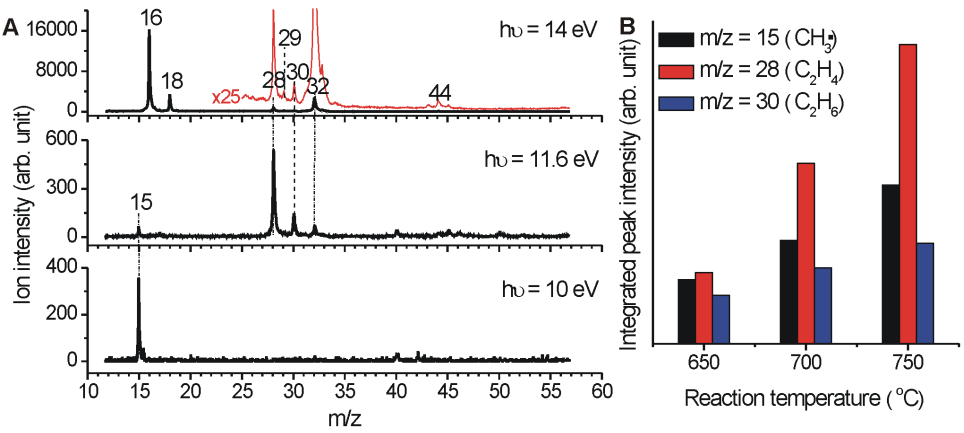

Figure 3 | (A) SVUV-PIMS spectra of the gas-phase components of OCM reaction catalyzed by 5.6%-Li/MgO at 750°C ionized with photons at different energies. (B) Integrated SVUV-PIMS peak intensity of gas-phase methyl radicals, ethylene and ethane during OCM reaction catalyzed by 5.6%-Li/MgO at 650, 700 and 750°C.

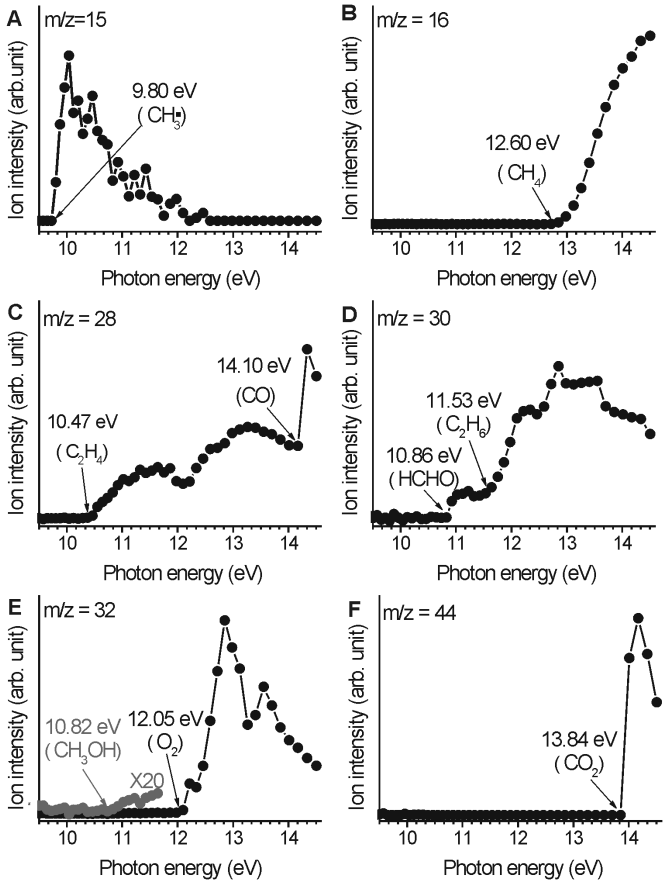

Figure 4 | Photoionization efficiency spectra of m/z = 15 (A), 16 (B), 28 (C), 30 (D), 32 (E) and 44 (F) in the SVUV-PIMS spectra of the gas-phase components of OCM reaction catalyzed by 5.6%-Li/MgO at 750°C.

the gas-phase components of OCM reaction catalyzed by 5.6%-Li/MgO catalyst at various temperatures ionized with photons at 10.0 and 11.6 eV, and Figure 3B compares the concentrations of gas-phase methyl radical, ethylene and ethane. The concentrations of gas-phase methyl radical, ethylene and ethane simultaneously increase with the reaction temperature. Figure S5 shows SVUV-PIMS spectra of the gas-phase components of OCM reaction catalyzed by 1.3%-Li/MgO and 5.6%-Li/MgO catalysts at 750°C with photons at 10.0 and 11.6 eV, and Figure 5B compares the concentrations of gas-phase methyl radical, ethylene and ethane. 5.6%-Li/MgO catalyst is more catalytically active than 1.3%-Li/MgO, and the concentrations of gas-phase methyl radical, ethylene and ethane in the OCM reaction catalyzed by 5.6%-Li/MgO are larger than those catalyzed by 1.3%-Li/MgO.

We analyzed the composition of Li/MgO catalysts after the activation in pure O_2 at 450°C for 2 hours and those after the catalytic performance evaluation in the OCM reaction up to 750°C (Table 1). After the activation in pure O_2 at 450°C for 2 hours, the Li amount in 1.3%-Li/MgO only slightly decreases from 0.21% to 0.18% but the Li amount in 5.6%-Li/MgO substantially decreases from 1.16% to 0.17%. This demonstrates that the treating condition strongly affects the composition of Li/MgO catalysts. The Li amount in Li/MgO catalysts after the O_2 activation does not decrease much even after the catalytic performance evaluation in the OCM reaction up to 750°C. Thus 1.3%-Li/MgO and 5.6%-Li/MgO catalysts under the working condition actually have similar amounts of Li. We employed TEM and HRTEM to examine the morphology and microstructure of as prepared Li/MgO, Li/MgO activated in pure O_2 at 450°C for 2 hours, and Li/MgO after the catalytic performance evaluation in the OCM reaction up to 750°C. TEM images (Figure S6) demonstrate that the grain size of catalyst particles in 5.6%-Li/MgO are larger in 1.3%-Li/MgO. This agrees with the observation that the specific surface area of 1.3%-Li/MgO is larger than that of 5.6%-Li/MgO catalyst. As seen in the HRTEM images and the corresponding Fourier-transformed patterns (Figure 6), as prepared 1.3%-Li/MgO and 5.6%-Li/MgO catalysts exhibit similar morphologies. After the oxygen activation and catalytic performance evaluation, 1.3%-Li/MgO catalysts exhibit quite regular morphologies mainly consisting of stepped terraces with the lattice fringe corresponding to MgO(200); 5.6%-Li/MgO catalysts are with irregular morphologies within which the lattice fringe corresponding to MgO(111) is visible. Thus, although 1.3%-Li/MgO and 5.6%-Li/MgO under the OCM reaction condition are with similar Li amounts (~0.16%), they exhibit different morphologies and microstructures.

Discussion

The SVUV-PIMS spectroscopy online detects the presence of species with m/z = 15 in the gas-phase components during the OCM reaction catalyzed by Li/MgO catalysts, and by measuring its ionization threshold, unambiguously identifies this species to be methyl radical. Without the catalysts, no methyl radical was detected by SVUV-PIMS under the same reaction condition. These results clearly prove the generation of gas-phase methyl radicals by the activation of methane on the Li/MgO catalyst surface during the OCM reaction. Comparing previous MIESR results[8–17], our SVUV-PIMS results represent a direct and unambiguous detection of surface-generated,

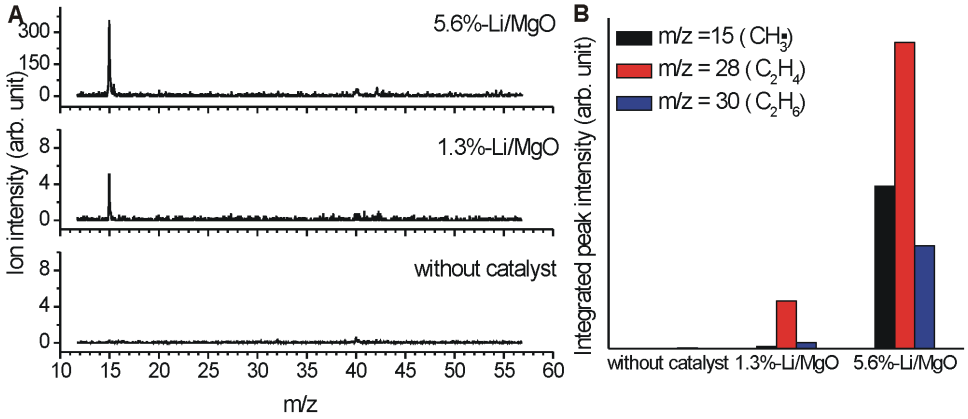

Figure 5 | (A) SVUV-PIMS spectra of the gas-phase components of OCM reaction catalyzed by various catalysts at 750°C ionized with photons at 10.0 eV. (B) Integrated SVUV-PIMS peak intensity of gas-phase methyl radicals, ethylene and ethane during OCM reaction catalyzed by various catalysts at 750°C.

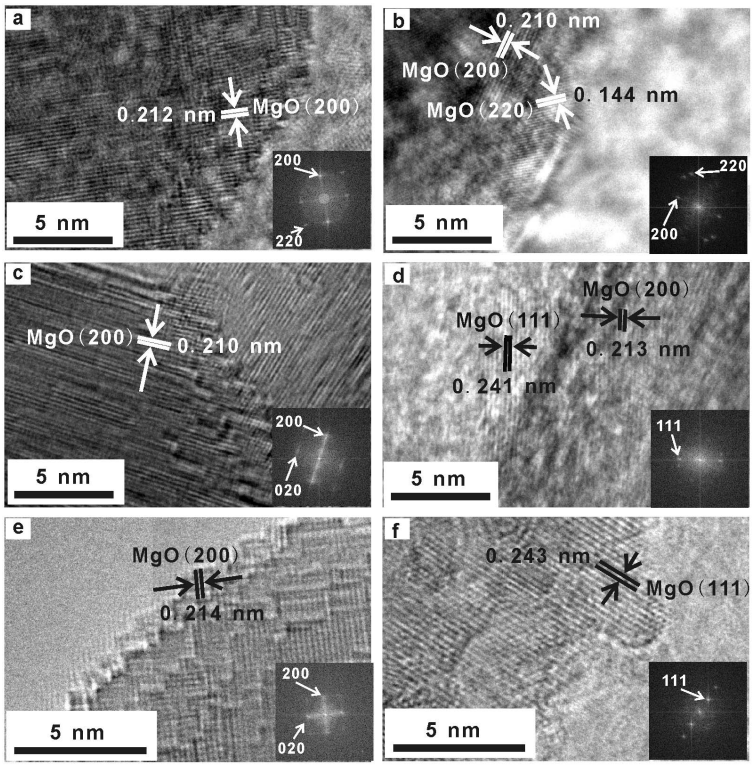

Figure 6 | High-resolution TEM images of as prepared 1.3%-Li/MgO (a) and 5.6%-Li/MgO (b), as-prepared 1.3%-Li/MgO (c) and 5.6%-Li/MgO (d) activated in pure O_2 at 450°C for 2 hours, as-prepared 1.3%-Li/MgO (e) and 5.6%-Li/MgO (f) after the catalytic performance evaluation in the OCM reaction up to 750°C. The inset shows the Fourier-transformed pattern of HRTEM image.

gas-phase methyl radicals in the OCM reaction catalyzed by Li/MgO catalysts. Moreover, the simultaneous analysis of gas-phase components by SVUV-PIMS spectroscopy enables the clear correlation among the concentrations of gas-phase methyl radical, ethylene and ethane in the OCM reaction catalyzed by Li/MgO catalysts. Our results show that the gas-phase concentration of ethylene and ethane varies in the same trend to the gas-phase concentration of methyl radical, suggesting that ethylene and ethane should be products of secondary reactions of methyl radicals. Meanwhile, the gas-phase concentration of ethylene and ethane detected by SVUV-PIMS spectroscopy in the OCM reaction operated under a total pressure of 4 torr varies in the same trend to the yield of ethylene and ethane measured in an ambient-pressure catalytic reactor, indicating that the results acquired by the SVUV-PIMS study of the OCM reaction under a total pressure of 4 torr should be applicable for the practical OCM reaction. Thus, our SVUV-PIMS results provide direct and unambiguous experimental evidence for the OCM reaction mechanism that the OCM reaction is initiated via the activation of methane on the catalyst surface to generate methyl radicals followed by the secondary reactions of methyl radicals[5,7].

Although 1.3%-Li/MgO and 5.6%-Li/MgO under the OCM reaction condition are with similar Li amounts (~0.16%), 5.6%-Li/MgO exhibits a much better catalytic performance in the OCM reaction than 1.3%-Li/MgO. Two schools of thought exist in assigning the role of Li in Li/MgO catalysts for the OCM reaction: forming Li^+O^- sites[3] or forming MgO defect sites such as F centers[38,39]. Recently the segregation Li in Li/MgO catalysts and the subsequent desorption of Li from Li/MgO catalysts during the OCM reaction were observed to strongly affect the morphology and microstructure of MgO[30,40]. Our TEM and HRTEM results demonstrate that 1.3%-Li/MgO and 5.6%-Li/MgO exhibit different morphologies and microstructures. 5.6%-Li/MgO exhibits a more irregular morphology than 1.3%-Li/MgO and thus likely exposes more defect sites; meanwhile, 1.3%-Li/MgO mainly exposes {100} crystal planes whereas crystal planes other than {100}, such as {111} crystal planes, are exposed on 5.6%-Li/MgO. Among various crystal planes of fcc MgO, MgO(100) surface is thermodynamically most stable. Thus, high-energetic crystal planes and a high density of defect sites exposed on Li/MgO catalyst are beneficial for the OCM reaction. The restructuring process resulting in the different morphologies and microstructures of 1.3%-Li/MgO and 5.6%-Li/MgO catalysts likely occurs during the activation process in pure O_2 at 450°C for 2 hours. After the activation process, as-prepared 1.3%-Li/MgO catalyst containing only 0.21% adopts quite regular morphologies mainly consisting of stepped terraces exposing thermodynamically most stable {100} crystal planes, but as-prepared 5.6%-Li/MgO catalyst containing 1.16% Li adopts irregular morphologies exposing high-energetic crystal planes and a high density of defect sites, and the Li amount decreases to 0.17%. These observations suggest that the presence of sufficient amount of Li in Li/MgO during the oxygen activation process and its segregation and subsequent desorption play a critical role in forming the morphology exposing high-energetic crystal planes and a high density of defect sites. The amount of Li, the oxygen pressure and the temperature seem to the major factors affecting the restructuring process of Li/MgO catalyst. Thus it deserves further efforts to optimize the condition of oxygen activation process to engineer the morphology and microstructure of Li/MgO active in the OCM reaction.

In summary, employing synchrotron VUV photoionization mass spectroscopy, we have directly and unambiguously detected methyl radicals in the oxidative coupling of methane catalyzed by Li/MgO catalysts and confirmed the OCM reaction mechanism that the OCM reaction is initiated via the activation of methane on the catalyst surface to generate methyl radicals. We have also revealed the critical role of Li additive in forming Li/MgO catalyst exposing high-energetic crystal planes and a high density of defect sites that are beneficial for the OCM reaction. These findings greatly deepen our fundamental understanding of the reaction mechanism and

structure-activity relationship of the OCM reaction and will help to design new well-performing OCM catalytic materials.

Methods

MgO (AR, > 98.5%) and Li_2CO_3 (AR, >98.5%) were purchased from Sinopharm Chemical Reagent Co., Ltd. and used as received. Distilled water was made by Water Purifier lab pure water system. All gases were with ultrahigh purity and were obtained from Nanjing Shangyuan Industrial Gas Factory, China.

Li/MgO catalysts were prepared by addition of 2.5 g MgO and calculated amounts of Li_2CO_3 into 100 mL distilled water. The mixture was adequately stirred at 60°C for 4 hours. The resulting precipitate was collected by centrifugation, baked at 60°C, and calcined in a Muffle furnace at 800°C for 4 hours.

Compositions of catalysts were analyzed by an Optima 7300 DV inductively coupled plasma atomic emission spectrometer (ICP-AES). N_2 adsorption-desorption isotherms were measured on a Beckman Coulter SA3100 surface area analyzer. Catalysts were degassed at 300°C in N_2 atmosphere prior to the measurements. XRD spectra were acquired on a Philips X'Pert PRO SUPER X-ray diffractometer with a Ni-filtered Cu Kα x-ray source (wavelength: 0.15418 nm) operating at 40 kV and 50 mA. Transmission electron microscopy (TEM) measurements were preformed on a JEOL-2100F microscope.

Catalytic performance of Li/MgO catalysts in oxidative coupling of methane was evaluated with an ambient-pressure fixed-bed flow reactor. 1 g catalyst (40–60 mesh) was loaded in a quartz reactor. The catalyst was activated in pure O_2 (flow rate: 50 mL/min) at 450°C for 2 hours and then switched to the reactants consisting of 8% CH_4 and 4% O_2 balanced with Ar (flow rate: 150 mL/min). The catalyst was heated to desired reaction temperatures and then kept for 30 min until the catalytic reaction reached a steady state. Then the composition of effluent gas was analyzed with two online GC-14 gas chromatographs. One was equipped with carbon-zeolite column and TCD detector for the separation and detection of CH_4, CO and CO_2; the other with Porapak Q column and H_2-flame ionization detector for the separation and detection of C_2H_4 and C_2H_6. The conversion of CH_4 was calculated from the change in CH_4 concentration in the inlet and outlet gases. The selectivity of C_2H_4 and C_2H_6 was calculated the twice amount of produced C_2H_4 or C_2H_6 divided by the amount of converted CH_4.

Synchrotron VUV photoionization mass spectroscopy (SVUV-PIMS) experiments were performed on the combustion station of National Synchrotron Radiation Laboratory (Hefei, China)[13]. A quartz catalytic reactor was designed to online connect the SVUV-PIMS spectrometer (Figure 1). The OCM reaction in this reactor was operated at a total pressure of 4 Torr, and the reactants, catalysts (2 mm × 2 mm) and the pretreatment are same as those employed in the ambient-pressure reactor. After the catalytic reaction reached a steady state at the desired temperature, the composition of effluent gas was analyzed by the online SVUV-PIMS spectrometer.

1. Keller, G. E. & Bhasin, M. M. Synthesis of ethylene via oxidative coupling of methane .1. determination of active catalysts. *J. Catal.* **73**, 9–19 (1982).
2. Lee, J. S. & Oyama, S. T. Oxidative coupling of methane to higher hydrocarbons. *Catal. Rev.* **30**, 249–280 (1988).
3. Lunsford, J. H. The catalytic oxidative coupling of methane. *Angew. Chem. Int. Edit.* **34**, 970–980 (1995).
4. Amenomiya, Y., Birss, V. I., Goledzinowski, M., Galuszka, J. & Sanger, A. R. Conversion of methane by oxidative coupling. *Catal. Rev.* **32**, 163–227 (1990).
5. Arndt, S. *et al.* A critical assessment of Li/MgO-based catalysts for the oxidative coupling of methane. *Catal. Rev.* **53**, 424–514 (2011).
6. Hammond, C., Conrad, S. & Hermans, I. Oxidative methane upgrading. *Chemsuschem* **5**, 1668–1686 (2012).
7. Ertl, G., Knözinger, H., Schüth, F. & Weitkamp, J. *Handbook of Heterogeneous Catalysis* (Wiley-VCH, 2008).
8. Driscoll, D. J., Martir, W., Wang, J. X. & Lunsford, J. H. Formation of gas-phase methyl radicals over MgO. *J. Am. Chem. Soc.* **107**, 58–63 (1985).
9. Lunsford, J. H. *et al.* The effect of chloride-ions on a Li^+-MgO catalyst for the oxidative coupling of methane. *J. Catal.* **147**, 301–310 (1994).
10. Campbell, K. D. & Lunsford, J. H. Contribution of gas-phase radical coupling in the catalytic-oxidation of methane. *J. Phys. Chem.* **92**, 5792–5796 (1988).
11. Tong, Y. D., Rosynek, M. P. & Lunsford, J. H. Secondary reactions of methyl radicals with lanthanide oxides - their role in the selective oxidation of methane. *J. Phys. Chem.* **93**, 2896–2898 (1989).
12. Xu, M. T. & Lunsford, J. H. Effect of temperature on methyl radical generation over Sr/La_2O_3 catalysts. *Catal. Lett.* **11**, 295–300 (1991).
13. Tong, Y. D. & Lunsford, J. H. Gas-phase coupling of methyl radicals during the partial oxidation of methane over transition-metal oxide catalysts. *J. Chem. Soc. Chem. Comm.* 792–793 (1990).
14. Zhang, H. S., Wang, J. X., Driscoll, D. J. & Lunsford, J. H. Activation and oxidative dimerization of methane over lithium-promoted zinc-oxide. *J. Catal.* **112**, 366–374 (1988).
15. Lin, C. H., Campbell, K. D., Wang, J. X. & Lunsford, J. H. Oxidative dimerization of methane over lanthanum oxide. *J. Phys. Chem.* **90**, 534–537 (1986).
16. Campbell, K. D., Zhang, H. & Lunsford, J. H. Methane activation by the lanthanide oxides. *J. Phys. Chem.* **92**, 750–753 (1988).
17. Campbell, K. D., Morales, E. & Lunsford, J. H. Gas-phase coupling of methyl radicals during the catalytic partial oxidation of methane. *J. Am. Chem. Soc.* **109**, 7900–7901 (1987).
18. Feng, Y., Niiranen, J. & Gutman, D. Kinetic-studies of the catalytic-oxidation of methane .1. methyl radical production on 1-percent Sr/La_2O_3. *J. Phys. Chem.* **95**, 6558–6563 (1991).
19. Horn, R. *et al.* Gas phase contributions to the catalytic formation of HCN from CH_4 and NH_3 over Pt: An in situ study by molecular beam mass spectrometry with threshold ionization. *Phys. Chem. Chem. Phys.* **6**, 4514–4521 (2004).
20. Geske, M., Pelzer, K., Horn, R., Jentoft, F. C. & Schlögl, R. In-situ investigation of gas phase radical chemistry in the catalytic partial oxidation of methane on Pt. *Catal. Today* **142**, 61–69 (2009).
21. Cool, T. A. *et al.* Selective detection of isomers with photoionization mass spectrometry for studies of hydrocarbon flame chemistry. *J. Chem. Phys.* **119**, 8356–8365 (2003).
22. Kohse-Höinghaus, K. *et al.* Biofuel combustion chemistry: from ethanol to biodiesel. *Angew. Chem. Int. Edit.* **49**, 3572–3597 (2010).
23. Battin-Leclerc, F. *et al.* Experimental confirmation of the low-temperature oxidation scheme of alkanes. *Angew. Chem. Int. Ed.* **49**, 3169–3172 (2010)
24. Li, Y. Y. & Qi, F. Recent applications of synchrotron vuv photoionization mass spectrometry: insight into combustion chemistry. *Accounts. Chem. Res.* **43**, 68–78 (2010).
25. Li, Y. *et al.* Effect of the pressure on the catalytic oxidation of volatile organic compounds over Ag/Al_2O_3 catalyst. *Appl. Catal. B* **89**, 659–664 (2009).
26. Bahlawane, N. *et al.* Nickel and nickel-based nanoalloy thin films from alcohol-assisted chemical vapor deposition. *Chem. Mater.* **22**, 92–100 (2010).
27. Liu, B. *et al.* Catalytic decomposition of methane on impregnated nickel based anodes with molecular-beam mass spectrometry and tunable synchrotron vacuum ultraviolet photoionization. *Int. J. Hydrogen Energy* **37**, 8354–8359 (2012).
28. Qi, F. *et al.* Isomeric identification of polycyclic aromatic hydrocarbons formed in combustion with tunable vacuum ultraviolet photoionization. *Rev. Sci. Instrum.* **77**, 084101 (2006).
29. Huang, C. Q. *et al.* Modification of photoionization mass spectrometer with synchrotron radiation as ionization source. *Rev. Sci. Instrum.* **76**, 126108 (2005).
30. Myrach, P. *et al.* Temperature-dependent morphology, magnetic and optical properties of Li-doped MgO. *ChemCatChem* **2**, 854–862 (2010).
31. Arndt, S. *et al.* Li-doped MgO from different preparative routes for the oxidative coupling of methane. *Top. Catal.* **54**, 1266–1285 (2011).
32. Linstrom, P. J. & Mallard, W. G. *NIST Chemistry Webbook*, National Institute of Standards and Technology, Gaithersburg, MD, **2008**; Number 69, http://webbook.nist.gov.
33. Mackie, R. A. *et al.* A photoionization mass spectrometric study of acetylene and ethylene in the VUV spectral region. *Int. J. Mass Spectrom.* **223–224**, 67–79 (2003).
34. Mackie, R. A. *et al.* The molecular and dissociative photoionization of ethane in the inner and outer valence energy regions. *J. Phys. B: Atom. Mol. Opt. Phys.* **35**, 1061–1069 (2002).
35. Traeger, J. C. & Mcloughlin, R. G. Absolute heats of formation for gas-phase cations. *J. Am. Chem. Soc.* **103**, 3647–3652 (1981).
36. Ito, T. & Lunsford, J. H. Synthesis of ethylene and ethane by partial oxidation of methane over lithium-doped magnesium-oxide. *Nature* **314**, 721–722 (1985).
37. Cool, T. A. *et al.* Studies of a fuel-rich propane flame with photoionization mass spectrometry. *P. Combust.Inst.* **30**, 1681–1688 (2005).
38. Wu, M. C., Truong, C. M., Coulter, K. & Goodman, D. W. Investigations of active-sites for methane activation in the oxidative coupling reaction over Pure and Li-Promoted MgO Catalysts. *J. Catal.* 1993.1089 (1993).
39. Wu, M. C., Truong, C. M., Coulter, K. & Goodman, D. W. Role of f-centers in the oxidative coupling of methane to ethane over Li-promoted MgO catalysts. *J. Am. Chem. Soc.* **114**, 7565–7567 (1992).
40. Zavyalova, U. *et al.* Morphology and microstructure of Li/MgO catalysts for the oxidative coupling of methane. *Chemcatchem* **3**, 949–959 (2011).

Acknowledgements

This work was financially supported by National Natural Science Foundation of China (21173204), National Basic Research Program of China (2013CB933104, 2010CB923301), Fundamental Research Funds for the Central Universities, and MPG-CAS partner group program.

Author contributions

W.H. and F.Q. designed the project and analyzed the data. L.L. carried out all experiments and analyzed the data. X.T., Y.W. and S.S. carried out the synchrotron VUV photoionization mass spectroscopy and analyzed the data. W.W. carried out the catalytic activity evaluation experiments and analyzed the data. W.H. wrote the paper, and all authors commented on the manuscript.

Additional information

Supplementary information accompanies this paper at http://www.nature.com/scientificreports

Competing financial interests: The authors declare no competing financial interests.

How to cite this article: Luo, L. *et al.* Methyl Radicals in Oxidative Coupling of Methane Directly Confirmed by Synchrotron VUV Photoionization Mass Spectroscopy. *Sci. Rep.* **3**, 1625; DOI:10.1038/srep01625 (2013).